

Virtual Time Horizon Control via Communication Network Design*

Zoltan Toroczkai[†]György Korniss[‡]Mark A. Novotny[§]Hasan Guclu[¶]

July 5, 2021

Abstract

We consider massively parallel discrete event simulations where the communication topology among the processing elements is a complex graph. In the case of regular topologies we review recent results on virtual time horizon management. First we analyze the computational scalability of the conservative massively parallel update scheme for discrete event simulations by using the analogy with a well-known surface growth model, then we show that a simple modification of the regular PE communication topology to a small-world topology will also ensure measurement scalability. This leads to a fully scalable parallel simulation for systems with asynchronous dynamics and short-range interactions. Finally, we present numerical results for the evolution of the virtual time horizon on scale-free Barabási-Albert networks serving as communication topology among the processing elements.

*Invited review paper for Volume on Computational Complexity and Statistical Physics, Santa Fe Institute Studies in the Sciences of Complexity series, Oxford University Press, 2003.

[†]Complex Systems Group, Theoretical Division, Los Alamos National Laboratory, MS-B213, Los Alamos, NM, 87545, USA. toro@lanl.gov

[‡]Department of Physics, Applied Physics, and Astronomy, Rensselaer Polytechnic Institute, 110 8th Street, Troy, NY 12180-3590 USA. korniss@rpi.edu

[§]Department of Physics and Astronomy and ERC, Mississippi State University, Mississippi State, MS 39762-5167 USA, novotny@erc.msstate.edu

[¶]Department of Physics, Applied Physics, and Astronomy, Rensselaer Polytechnic Institute, 110 8th Street, Troy, NY 12180-3590 USA. gucluh@rpi.edu

Key words: massively parallel discrete event simulations, surface growth, graphs, small world networks, power-law networks

1 Introduction to the scalability problem of massively parallel discrete-event simulations

The description and understanding of complex systems dynamics is in most cases impossible via analytic methods. The density of problems that are rigorously solvable with analytic tools is vanishingly small in the set of all problems. The only way one can obtain system level understanding of such problems is through direct simulation. The class of complex systems considered here are made of a large number of interacting individual elements with a finite number of attributes, or local state variables, each assuming a countable number (typically finite) of values. The dynamics of the local state variables are discrete events occurring in continuous time. Between two consecutive updates, the local variables stay unchanged. Another important assumption we make is that the interactions in the underlying system to be simulated have finite range. Examples of such systems include: magnetic systems (spin states and spin flip dynamics), surface growth via molecular beam epitaxy (height of the surface at a given point, measured from a growth level, molecular deposition and diffusion dynamics); epidemiology (health of an individual, health state change due to infection, or recovery); financial markets (wealth state, buy/sell dynamics), wireless communications, or queueing systems (number of jobs, job arrival dynamics).

Often, as the case studied here, the dynamics of such systems is inherently stochastic and *asynchronous*. The simulation of such systems is rather non-trivial and in most cases the complexity of the problem requires simulations on distributed architectures, defining the field of Parallel Discrete-Event Simulations (PDES) [1, 2, 3]. Conceptually, the computational task is divided among N processing elements (PE-s), where each processor evolves the dynamics of the allocated piece. Due to the interactions among the individual elements of the simulated system (spins, atoms, packets, calls, etc.) the PE-s must coordinate with a subset of other PE-s during the simulation. For example, the state of a spin can only be updated if the state of the neighbors is known. However, some neighbors might belong to the computational domain of another PE, thus message passing will be required in order to preserve causality. In the PDES schemes we analyze, update attempts are self-initiated [4] and are independent of the configuration of the underlying system [5, 6]. Although these properties simplify the analysis of the corresponding PDES schemes, they can be highly efficient [7] and are readily applicable to a large number problems in science and engineering. Further, the performance and the scalability of these PDES schemes become independent of the specific underlying system i.e., we learn the generic behavior of these complex computational schemes.

The update dynamics, together with the information sharing among PE-s, make the parallel discrete-event simulation process a complex dynamical system itself. In fact, it perfectly fits the type of complex systems we are considering here: the individual elements are the PE-s, and their states (local simulated time) evolve according to update events which are dependent on the states of the neighboring PE-s.

With the number and size of parallel computers on the rise, the problem of designing efficient parallel algorithms, or update schemes becomes increasingly important. In passing, we can mention a few examples of large parallel computers: the 9472-node ASCII Red at Sandia, the 12288-node QCDSF Teraflop Machine at Brookhaven, the 8192-node IBM ASCII White with 12.3 Teraflops. IBM is currently building the Blue Gene/L with 200

Teraflops, with over 10^6 nodes. As a matter of fact the largest supercomputer ever built is by Nature itself: the brain, which does an immense parallel computing task to sustain the individual. In particular the human brain has 10^{11} PE-s (neurons) each with an average of 10^4 synaptic connections, creating a bundle on the order of 10^{15} “wires” jammed into a volume of approximately 1400 cm^3 .

The design of efficient parallel update schemes is a rather challenging problem, due to the fact that the dynamics of the simulation scheme itself is a complex system, whose properties are hard to deduce using classical methods of algorithm analysis. Here we present a less conventional approach to the analysis of efficiency and scalability for the class of massively parallel conservative PDE-s schemes, by exactly mapping the parallel computational process itself onto a non-equilibrium surface growth model [8]. This allows us to translate the questions about efficiency and scalability into questions formulated in terms of certain topological properties of this non-equilibrium surface. Then, using methods from statistical mechanics, developed some time ago to study the dynamics of such surfaces (in a completely different context), we solve the scalability problem of the computational PDES-s scheme [8, 9]. Similar connections between computational schemes and complex systems behavior have recently been made [10, 11] for rollback-based PDES-s algorithms [12] and self-organized criticality [13].

Since one is interested in the *dynamics* of the underlying complex system, the PDES scheme must simulate the ‘physical time’ variable of the complex system. When the simulations are done on a single processor machine, a single (global) time stream is sufficient to “label” or time-stamp the updates of the local configurations, regardless whether the dynamics of the underlying system is synchronous or asynchronous. When simulating asynchronous dynamics on distributed architectures, however, each PE generates its own physical, or virtual time, which is the physical time variable of the particular computational domain handled by that PE. Due to the varying complexity of the computation at different PE-s, at a given wall-clock instant the simulated virtual times of the PE-s can differ, a phenomenon called “time horizon roughening”. We denote the simulated, or virtual time at PE i measured at wall-clock time t , by $\tau_i(t)$. For non-interacting subsystems the wall-clock time t is directly proportional to the (discrete) number of parallel steps simultaneously performed on each PE, also called the number of Monte-Carlo steps (MCS) in dynamic Monte Carlo simulations. Without altering the meaning, t from now on will be used to denote the number of discrete steps performed in the parallel simulation. The set of virtual times $\{\tau_i(t)\}_{i=1}^N$ forms the *virtual time horizon* of the PDES-s scheme after t parallel updates.

In conservative PDES-s schemes [14], a PE will only perform its next update if it can obtain the correct information to evolve the local configuration (local state) of the underlying physical system it simulates, without violating causality. Otherwise, it idles. Specifically, when the underlying system has nearest-neighbor interactions, each PE must check with its “neighboring” PEs (mimicking the interaction topology of the underlying system) to see if those are progressed at least up to the point in virtual time where the PE itself did [5, 6]. Based on the fundamental notion of discrete-event systems that the state of a local state variable remains unchanged between two successive update attempts, the above rule guarantees the causality of the simulated dynamics [5, 6]. A simple example illustrating this is shown in Figure 1. One can consider, for example, a magnetic system as the underlying physical system, where the spins are arranged in the sites of a one-dimensional lattice, and

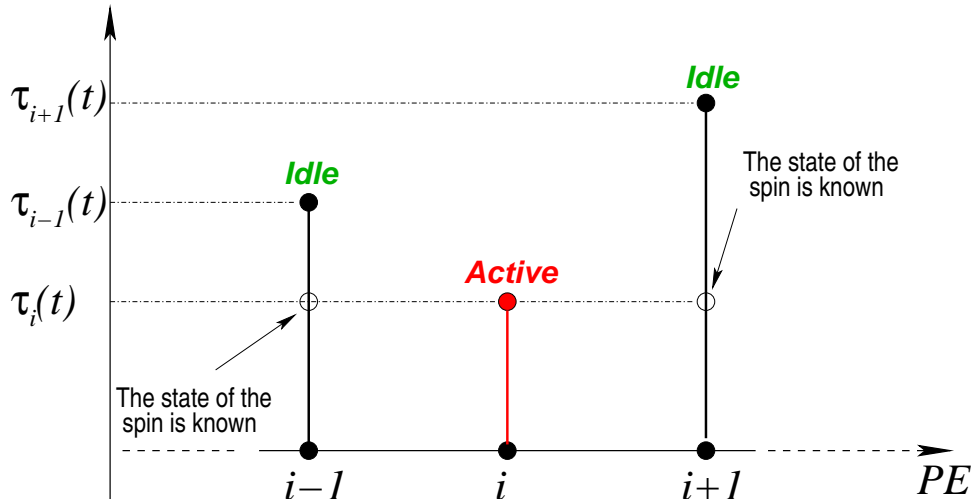


Figure 1: A simple diagram to illustrate the conservative PDES-s scheme for a one-dimensional system with nearest-neighbor interactions.

that a single spin is handled by a single PE (for more realistic and efficient implementations see [5, 6, 7]). In Fig. 1, which shows the distribution of the virtual simulated times at a given wall-clock instant t , the only PE that can update from the set $\{i-1, i, i+1\}$ is in site i , since the state of the neighboring spins at sites $i \pm 1$ are already known. However, PE-s $i \pm 1$ cannot update their spin states at wall clock instant t , because, the state of the neighboring spin i at *their* simulated times (at τ_{i-1} and τ_{i+1}) is not known yet. In other words PE i can only update at wall-clock instant t if $\tau_i(t) \leq \min\{\tau_{i-1}(t), \tau_{i+1}(t)\}$, i.e., its virtual time is a *local minimum* among the virtual times of its neighboring PE-s. It is easy to see that the same conclusion holds for arbitrary PE topologies. Let the topology for the communication among the processing elements be symbolized by a graph $G(V, E)$, where V is the vertex set of N nodes and E is the edge set of G . Given a node $i \in V(G)$, we denote by $S_i^{(1)}$ the set of first order neighbors on G of i . Then, node (PE) i can update its state, in the conservative PDES-s scheme iff:

$$\tau_i^{(G)}(t) \leq \min_{j \in S_i^{(1)}} \{\tau_j^{(G)}(t)\} \quad , i = 1, \dots, N. \quad (1)$$

In the following, the set of (active) nodes which obey condition (1) at time t , will be denoted by $\mathcal{A}(t)$. Now we are in the position to formulate the scalability problem of PDES-schemes for systems with asynchronous dynamics. For the PDES-s scheme to be fully scalable, the following two criteria must be met: (i) the virtual time horizon must progress on average at a nonzero rate, and (ii) the typical spread of the time horizon should be finite, as the number of PE-s N goes to infinity. When the first criterion is ensured for large enough times t , the simulation is said to be *computationally scalable*, and it just means that when increasing the size of the computation to infinity, while keeping the average computational domain/load on a single PE the same, the simulation will progress at a nonzero rate. However, as we will show below, increasing the system size, the *spread* in the time horizon can diverge, severely hindering frequent data collection about the state of the simulated system. Specifically, when one requires to take a measurement of some physical property of the simulated system at (virtual, or simulated) physical time τ , we have to *wait* (in wall-clock time) until all the

virtual simulated times at all the PE-s pass through the value of τ . Thus, in order to collect system-wide measurements from the simulation, we incur a waiting time proportional to the *spread*, or width of the fluctuating time horizon. For PDES-s schemes for which the spread diverges with system size, the waiting time for the measurements will also diverge, and the scheme is *not* measurement scalable. When condition (ii) is fulfilled for large enough times t , we say that the PDES-s scheme is *measurement scalable*.

The scalability criteria above can simply be formalized in terms of the properties of the virtual time horizon, $\{\tau_i^{(G)}(t)\}_{i=1}^N$. The average of the time horizon after t parallel steps is:

$$\bar{\tau}^{(G)}(t) = \frac{1}{N} \sum_{j=1}^N \tau_j^{(G)}(t) . \quad (2)$$

At a given (wall-clock) time t the only PE-s that can make progress, i.e., are not in idle, are those which have simulated virtual times obeying condition (1). Thus, the rate of progress of the time horizon average becomes:

$$\bar{\tau}^{(G)}(t+1) - \bar{\tau}^{(G)}(t) = \frac{1}{N} \sum_{l \in \mathcal{A}(t)} \left[\tau_l^{(G)}(t+1) - \tau_l^{(G)}(t) \right] . \quad (3)$$

The difference in the square brackets on the r.h.s of (3) is the *physical time* elapsed between two consecutive events in the physical domain simulated by the l th PE, and it is determined by the physical process responsible for the stochastic dynamics of the simulated complex system. If we replace the time intervals in square brackets in (3) with their (obviously finite) average value Δ , we obtain that the average progress rate of the time horizon, or average *utilization* $\langle u^{(G)}(t) \rangle = \langle \bar{\tau}^{(G)}(t+1) - \bar{\tau}^{(G)}(t) \rangle$ is proportional to the *number* of non-idling, or active PE-s. The average $\langle \cdot \rangle$ is taken over the stochastic event dynamics, which is assumed to be the same at all sites. For many cases, the Δ factor is independent on N (due to the finite range of the interaction in the complex system), so the computational efficiency, or average utilization of the simulation can simply be identified with the average density of the active PE-s:

$$\langle u^{(G)}(t) \rangle = \frac{\langle |\mathcal{A}^{(G)}(t)| \rangle}{N} \quad (4)$$

where $|\mathcal{A}^{(G)}(t)|$ denotes the number of elements of the set $\mathcal{A}^{(G)}(t)$. Thus, the PDES-s scheme is computationally scalable, if there exists a *constant* $c > 0$, such that:

$$\langle u^{(G)}(\infty) \rangle = \lim_{\substack{t \rightarrow \infty \\ N \rightarrow \infty}} \frac{\langle |\mathcal{A}^{(G)}(t)| \rangle}{N} > c. \quad (5)$$

The measurement scalability of the PDES-s scheme, is characterized by the spread of the virtual time horizon. Instead of dealing with the actual spread (difference between the maximum and minimum values) we shall consider the average “width” of the time horizon defined as:

$$\langle [w^{(G)}]^2(t) \rangle = \frac{1}{N} \sum_{j=1}^N \left[\tau_j^{(G)}(t) - \bar{\tau}^{(G)}(t) \right]^2 . \quad (6)$$

A PDES-s scheme is measurement scalable, if there exists a *constant* $M > 0$, such:

$$\langle [w^{(G)}]^2(\infty) \rangle = \lim_{\substack{t \rightarrow \infty \\ N \rightarrow \infty}} \frac{1}{N} \sum_{j=1}^N \left[\tau_j^{(G)}(t) - \bar{\tau}^{(G)}(t) \right]^2 < M. \quad (7)$$

In reality, the number of PEs N or the simulation time t can never be taken to infinity, so for practical purposes, the scalability is deduced from the scaling behavior of the quantities for long times and for large number of PEs. The setup presented above is perfectly suitable to establish a mapping between non-equilibrium surface growth models [19] and conservative PDES-s schemes. We discuss extensively this mapping in the next section.

The paper is organized as follows: in Section 2 we discuss the scalability of the computational phase and the failure of scalability of the measurement phase of the basic conservative scheme on regular topologies. Then we show how a simple modification of the communication topology (from a regular lattice to a small-world structure) leads to a fully scalable PDES-s scheme. In section 3 we study the scalability problem on scale-free network topologies. Section 4 is devoted to conclusions.

2 Scalability of conservative PDES-s schemes on regular and small-world topologies

In many large complex systems the stochastic event dynamics can be characterized by a Poisson distributed stream. For example, in an Ising magnet with single spin-flip Glauber dynamics [7] the spin-flip attempts are Poisson distributed events, or in wireless cellular communications the call arrivals also obey Poisson statistics [15], etc. In the following we restrict ourselves to such Poisson distributed stochastic processes for event dynamics, however numerical simulations show, that our conclusions for scalability hold for a large class of other stochastic distributions, as well. The evolution of the virtual time horizon incorporating condition (1) for Poisson asynchrony is given by the equation:

$$\tau_i^{(G)}(t+1) = \tau_i^{(G)}(t) + \eta_i(t) \prod_{j \in S_i^{(1)}} \theta(\tau_j^{(G)}(t) - \tau_i^{(G)}(t)) \quad (8)$$

Here $\theta(x)$ is the Heaviside step function, and $\eta_i(t)$ the Poisson distributed virtual time increment at PE i , and time t is. These increments are drawn at random, independently of i and t , and of the existing time horizon.

2.1 The basic conservative scheme on regular topologies

Next, we consider the *basic* conservative scheme, which is defined on regular, square lattice communication topologies, in d dimensions, so that $N = L^d$. For brevity, we drop from the superscript (G) in the notation for $\tau_i(t)$. In particular, we first illustrate our analysis on the simplest regular topology, that of a regular one-dimensional lattice, with periodic boundary conditions (G is a ring). Later we discuss the general, d -dimensional case. The evolution equation on the ring becomes simply:

$$\tau_i(t+1) = \tau_i(t) + \eta_i(t) \theta(\tau_{i-1}(t) - \tau_i(t)) \theta(\tau_{i+1}(t) - \tau_i(t)). \quad (9)$$

with the boundary conditions $\tau_{N+1} = \tau_N = \tau_0$. The total number of active sites/PE-s is thus given by $|\mathcal{A}(t)| = \sum_{i=1}^N \theta(\tau_{i-1}(t) - \tau_i(t))\theta(\tau_{i+1}(t) - \tau_i(t))$ so the average utilization (4) becomes:

$$\langle u(L, t) \rangle = \frac{1}{N} \sum_{i=1}^N \langle \theta(\tau_{i-1}(t) - \tau_i(t))\theta(\tau_{i+1}(t) - \tau_i(t)) \rangle \quad (10)$$

The average $\langle \cdot \rangle$ is performed over the random variables $\{\eta_i(t')\}_{i=1, \dots, L}^{t'=1, \dots, t}$ which have an exponential distribution, $Prob\{x < \eta \leq x + \delta x\} = \int_x^{x+\delta x} dy e^{-y}$. In spite of the simple appearance of the dynamics (9), and the exponential (or Poisson) stochastic dynamics at nodes, calculating the average utilization (10) is very difficult. Even a rigorous proof for the existence of the lower bound (5) using direct methods is still an open problem.

Here we present a different approach, by mapping first the problem to a non-equilibrium surface grown via molecular beam epitaxy (where atoms or molecules are deposited from vapors, or beams onto the surface) model. The quantities brought in analogy are: the i -th PE is the site i in the substrate; the number of parallel updates t is the number of deposited monolayers; $\tau_i(t)$ is the height $h_i(t)$ at site i and time t ; a virtual time increment of $\eta_i(t)$ at PE i in the t -th step, corresponds to a material “rod” of length $\eta_i(t)$ deposited onto the surface, see Figure (2). The length of the rod is a Poisson distributed random variable. During the t -th update, the rods are deposited only in *local minima* of the surface. The utilization of the PDES-s scheme corresponds to the the *density* of local minima of the growing surface. Even though the length of the rods are random independent variables, the fact that they can only be deposited in local minima will generate lateral correlations into the surface fluctuations, and makes the problem hard to compute exactly. The rods are

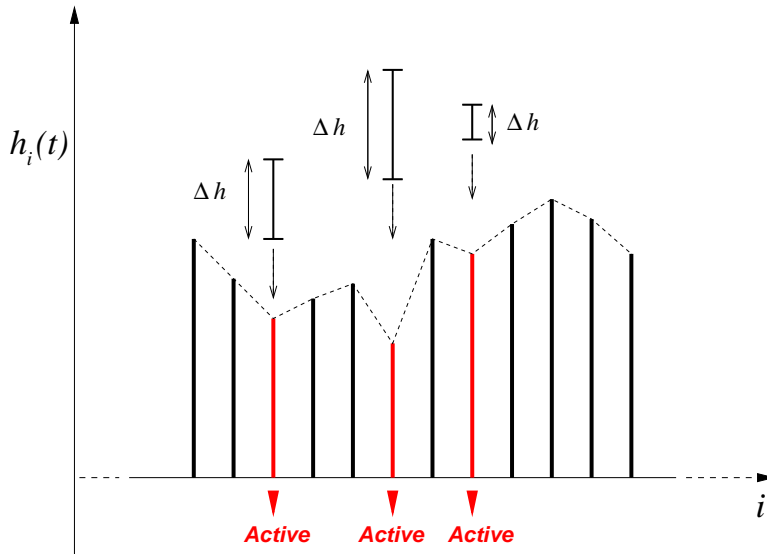


Figure 2: A simple surface growth model on a 1- d substrate corresponding to the basic conservative PDES-s scheme.

deposited onto the surface in a parallel update scheme: after all local minima are updated (deposited onto) the the time t is incremented by unity. We will coin the surface growth analog of our basic conservative PDES-s scheme , the ‘MPEU’ model (Massively Parallel Exponential Update Model).

Both the utilization (density of minima) and the width of the time horizon are quantities characterizing the fluctuations of the growing surface. The type of fluctuations can be classified into universality classes, each class having distinct statistical properties. Studying the PDES-s scheme as a surface growth model, we can describe its fluctuations and identify the surface growth universality class it belongs to. In order to do that we first introduce the slope variables, $\phi_i = \tau_i - \tau_{i-1}$. Provided $\tau_i(t)$ is a local minimum, a rod deposited of length η_i corresponds to taking an amount of η_i from ϕ_{i+1} and adding it to ϕ_i , since $\phi_i(t+1) = \tau_i(t) - \tau_{i-1}(t) + \eta_i(t)$ and $\phi_{i+1}(t+1) = \tau_{i+1}(t) - \tau_i(t) - \eta_i(t)$, i.e., in the *surface of slopes*, $\{\phi_i\}_{i=1}^L$ the dynamics is *biased surface diffusion*, given by the equation:

$$\phi_i(t+1) - \phi_i(t) = \eta_i(t)\theta(-\phi_i(t))\theta(\phi_{i+1}(t)) - \eta_{i-1}(t)\theta(-\phi_{i-1}(t))\theta(\phi_i(t)) \quad (11)$$

with the constraint $\sum_{i=1}^L \phi_i = 0$ generated by the periodic boundary conditions in the τ variables. In terms of the local slope variables, the expression for the average density of minima, or average utilization becomes: $\langle u(L, t) \rangle = \frac{1}{L} \sum_{i=1}^L \langle \theta(-\phi_i(t))\theta(\phi_{i+1}(t)) \rangle$. Translational invariance implies (no node is statistically special) $\langle u(L, t) \rangle = \langle \theta(-\phi_i(t))\theta(\phi_{i+1}(t)) \rangle$ for any $i = 1, 2, \dots, L$. From (9) it follows that $\langle \tau_i(t+1) \rangle - \langle \tau_i(t) \rangle = \langle u(L, t) \rangle$, thus, *the average rate of propagation of the MPEU surface is identical to the average utilization of the PDES-s scheme*. It is also easy to see that in the slope language it is identical to the average current in the ring. Next we perform a naive coarse graining by using the representation $\theta(\phi) = \lim_{\kappa \rightarrow 0} \frac{1}{2} [1 + \tanh(\phi/\kappa)]$, and keeping only the terms up to the order (ϕ/κ) . Performing this coarse graining, one obtains:

$$\langle \phi_i(t+1) \rangle - \langle \phi_i(t) \rangle = \frac{1}{4\kappa} \langle \phi_{i+1}(t) - 2\phi_i(t) + \phi_{i-1}(t) \rangle - \frac{1}{4\kappa^2} \langle \phi_i(\phi_{i+1} - \phi_{i-1}) \rangle. \quad (12)$$

Strictly speaking all of the $(\phi/\kappa)^n$, $n = 1, 2, \dots$ terms are divergent, but taking the proper continuum limit and introducing an appropriately scaled bias, the only relevant terms can be shown to be those appearing in Eq. (12) [16]. In the continuum limit, one thus, obtains for the coarse-grained field:

$$\frac{\partial}{\partial t} \hat{\phi} = \frac{\partial^2}{\partial x^2} \hat{\phi} - \lambda \frac{\partial}{\partial x} \hat{\phi}^2 \quad (13)$$

where λ is a parameter related to the coarse-graining procedure. The above nonlinear partial differential equation (13) is known as the nonlinear biased diffusion, or the Burgers equation [17]. Returning to the coarse-grained equivalent of the height, or virtual times, $\hat{\tau}$, via $\hat{\phi} = \partial \hat{\tau} / \partial x$, we obtain the Kardar-Parisi-Zhang (KPZ) equation [18]:

$$\frac{\partial \hat{\tau}}{\partial t} = \frac{\partial^2 \hat{\tau}}{\partial x^2} - \lambda \left(\frac{\partial \hat{\tau}}{\partial x} \right)^2. \quad (14)$$

To capture the fluctuations, one typically adds a delta-correlated noise term $\xi(x, t)$, to the right hand side, conserved for Eq. (13) (i.e., $\int \xi dx = 0$), and non-conserved for Eq. (14). It is important to note that we obtained the KPZ equation as a result of a coarse-graining procedure. While this results in the “loss” of some of the microscopic details for the original growth model on the lattice, Eq. (14) with noise added captures the long-wavelength behavior of the MPEU model. Thus, we claim that virtual time horizon for the basic conservative PDES scheme exhibit kinetic roughening and it belongs to the KPZ universality class. Identifying the universality class of a model is one of the main objectives and used extensively in

surface science to classify fluctuation statistics. Our procedure above indicates that the long-wavelength statistics of the fluctuations of the time horizon for the basic conservative PDES-s scheme is in fact captured by the nonlinear KPZ equation. In one dimension a steady-state for the surface fluctuations is reached (in the long time limit) for any *finite* system-size and it is governed by the Edwards-Wilkinson (EW) Hamiltonian $\mathcal{H}_{EW} \propto \int dx \left(\frac{\partial \hat{x}}{\partial x}\right)^2$ (see, e.g., [19]). The corresponding surface is a simple random-walk surface, where the slopes are independent random variables in the steady state. This means that out of the four local configurations of slopes around a point (down-up, down-down, up-up, up-down) only one contributes in average to a minimum (down-up), and since they are all equally likely, we conclude that $\langle u_{EW}(L \rightarrow \infty, t \rightarrow \infty) \rangle = 1/4 = 0.25$. Our numerical simulations for the MPEU model, see Fig.3a) indicate a value of $\langle u(L \rightarrow \infty, t \rightarrow \infty) \rangle = 0.24641 \pm (7 \times 10^{-6})$ a value close, but definitively not the same as for the simple random walk surface. The reason for the obvious difference is that the coarse-grained version and the original microscopic model are not identical over the whole spectrum of wavelengths of the fluctuations. The coarse-graining procedure preserves the statistics of the long-wavelength modes, but it

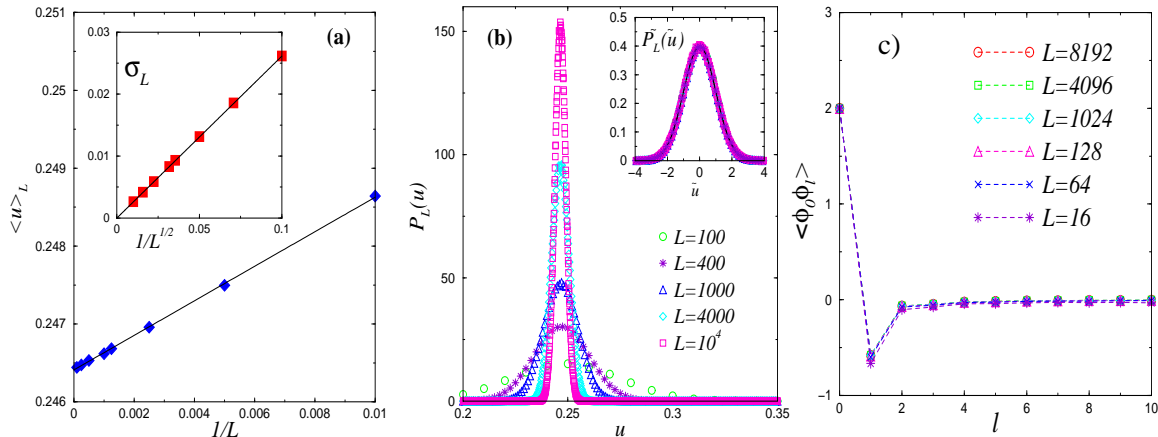


Figure 3: a) Steady state average utilization as a function of the number of PE-s L in a one-dimensional ring geometry; b) shows that the full distribution for the rescaled utilization in the steady state $\tilde{u} = (u(L) - \langle u(L) \rangle) / \sigma_L$ can be collapsed onto the normal distribution. c) Slope-slope correlation function.

loses some information on the short-wavelength ones. In particular the density of minima is heavily influenced by the short wavelengths (by how “fuzzy” the interface is). However, the density of minima cannot vanish in the thermodynamic limit: a zero density of local minima would imply that it is zero on all length-scales which would contradict the fact that it belongs to the EW universality class. The fact that the steady-state of the MPEU model belongs to the EW universality class guarantees that the local slopes are *short-range* correlated [Fig.3c)], and that the finite-size corrections for the density of local minima (average propagation rate of the surface) follows a universal scaling form [20]:

$$\langle u(L, \infty) \rangle \simeq \langle u(\infty, \infty) \rangle + \frac{\text{const.}}{L^{2(1-\alpha)}} . \quad (15)$$

Here α is the roughness exponent (equals to 1/2 for the EW universality class), characterizing the macroscopic surface-height fluctuations, as described in detail in the next paragraph.

Figure 3 confirms this scaling behavior. Further, calculating the spread in the average utilization the steady state as function of system size, $\sigma_L^2 = \langle u^2(L, \infty) \rangle - \langle u(L, \infty) \rangle^2$, we obtain $\sigma_L \propto L^{-1/2}$. These findings suggest that the utilization is a self-averaging macroscopic quantity: its full distribution $P_L(u)$ for large L is a Gaussian [Fig. 3b)].

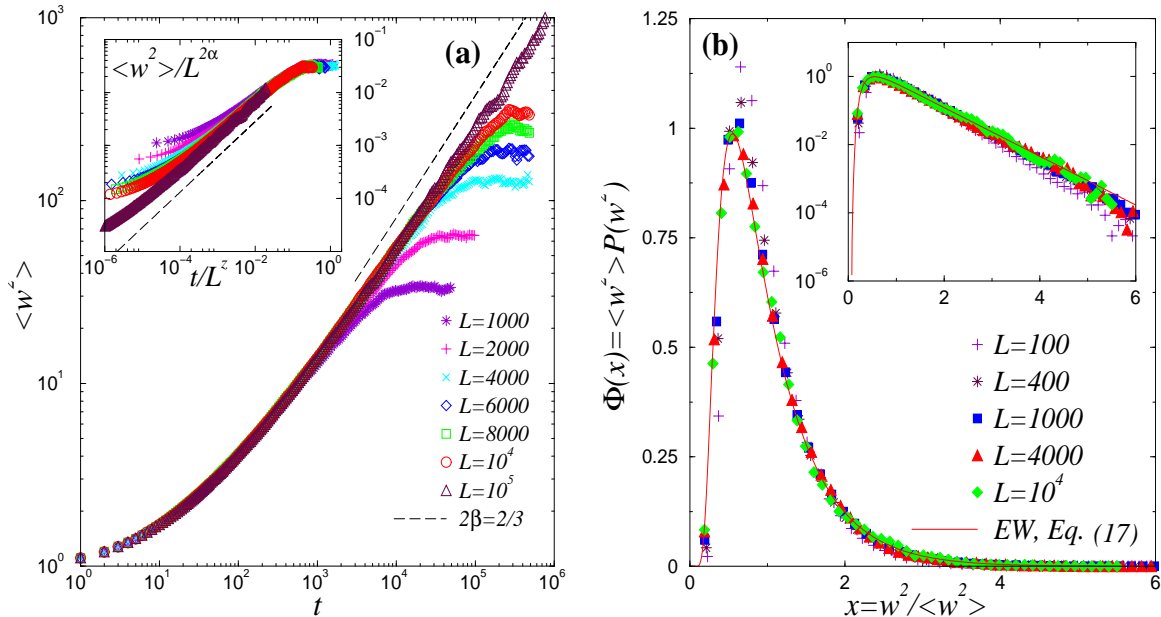


Figure 4: a) The width of the time horizon fluctuations show dynamical scaling and indicate KPZ universality. b) The scaling function for the steady-state width distribution follows the scaling function for the EW (one-dimensional KPZ) universality class.

In the following we show numerical results supporting our claim that the MPEU model belongs to the KPZ universality class. One of the fundamental characteristic quantities strongly influenced by the long-wavelength modes is the average width of the height fluctuations, as given in Eq. (6). As the surface grows due to deposition, after an initial transient the growth of the width will grow as a power law $\langle w^2(L, t) \rangle \sim t^{2\beta}$ along with the lateral surface correlations $\xi_{\parallel}(L, t) \sim t^{1/z}$, until the correlations reach the system size ($\xi_{\parallel} = L$) at a crossover time t_{\times} (see, e.g., Ref. [19]). After the crossover time t_{\times} (for any finite system L) the surface fluctuations are governed by a steady-state distribution and the width scales as

$$\langle w^2(L, \infty) \rangle \sim L^{2\alpha}. \quad (16)$$

The exponent β is called the growth exponent, α is called roughness exponent and z is called the dynamic exponent in the surface growth literature [19]. It is easy to show that the three exponents are not all independent, and $\alpha = z\beta$ holds [19]. Also, these scaling forms allow one to collapse all the different curves for the width onto a single function in the scaling regime, expressing the *dynamic scaling property* of the width: $\langle w^2(L, t) \rangle = L^{2\alpha} f(t/L^z)$ (f is easy to read of after comparing it to the scaling behavior). For the KPZ interface, the analytically obtained exact values for the exponents are: $\beta = 1/3$, $\alpha = 1/2$ and $z = 3/2$. Fig. 4 shows the numerically measured scaling properties for the width of the MPEU model. the numerically obtained values for the exponents $\beta = 0.326 \pm 0.005$, $\alpha = 0.49 \pm 0.01$ for

large system sizes ($L = 10^5$) confirm the KPZ behavior, including the dynamical scaling property (inset). Another confirmation for the EW universality class in the steady state, comes from measuring the full width distribution $P(w^2)$. For systems belonging to the EW universality class and having the same type of boundary conditions imposed, the width distribution has a universal scaling form[21] $P(w^2) = \frac{1}{\langle w^2 \rangle} \Phi\left(\frac{w^2}{\langle w^2 \rangle}\right)$ with

$$\Phi(x) = \frac{\pi^2}{3} \sum_{n=1}^{\infty} (-1)^{n-1} n^2 e^{-\frac{\pi^2}{6} n^2 x} , \quad (17)$$

where the above scaled distribution is for the case of periodic boundary conditions. Figure 4b) is a confirmation that MPEU indeed belongs to the steady state of the EW class, implying that the average utilization (density of local minima) approaches a non-zero, finite value in the thermodynamic limit (5) as reflected by Eq. (15). Therefore, the basic conservative scheme is *computationally scalable*. [For an in-depth and systematic analytical calculation of the density of minima (utilization) for a number of surface growth models (including the EW class) see Ref. [22].] The measurement phase of the basic conservative scheme, however, is *not* scalable, as indicated by the power-law divergence of the width in the long-time large L limit, Eq. (16). For higher-dimensional topologies, using universality arguments, the conclusion remains the same: the basic conservative PDES-s is computationally scalable, but the measurement phase may not be, depending on the upper critical dimension [19] of the surface (see Ref. [23, 24]).

2.2 The conservative scheme on small world networks

From the previous section it follows that the average width of the fluctuations scales in the steady state as $\langle w^2(L, t=\infty) \rangle \sim L^{2\alpha} = L$, i.e., it grows linearly with the system size. This means that the basic conservative PDES-s scheme is *not* measurement scalable. Standard methods to control the width of the virtual time horizon in a PDES scheme utilize some kind of a windowing technique [1]. That is, the height of the local simulated time at any PE cannot progress beyond an appropriately chosen and regularly updated “cap”, measured from the global minimum of the time horizon [25]. Thus, a PDES scheme with a moving window relies on frequent global synchronizations or communications, which, depending on the architecture, can get costly for large number of PEs. Here we show how to modify the original conservative scheme such that the scheme is also measurement scalable *without* global “intervention” [9].

The divergence of the width of the surface fluctuations is closely related to the fact that the lateral surface correlations also grow with the system size. In particular, for the one-dimensional EW surface in the steady state, for large L (and fixed l)

$$\langle \hat{\tau}_i \hat{\tau}_{i+l} \rangle \propto \xi_{||}(L, \infty) - |l| , \quad (18)$$

where $\hat{\tau}_i$ are the coarse-grained height fluctuations measured from the mean and $\xi_{||}(L, \infty) \sim L$. Thus, $\langle w^2(L, \infty) \rangle = \langle \hat{\tau}_i^2 \rangle \propto \xi_{||}(L, \infty) \sim L$. The “height-height” correlations can be characterized by introducing the structure factor for the heights:

$$S^{(\tau)}(k) = \frac{1}{L} \langle \tilde{\tau}_k \tilde{\tau}_{-k} \rangle \quad (19)$$

where $k = 2\pi n/L$, $n = 0, 1, 2, \dots, L-1$ is the wave-vector, and $\tilde{\tau}_k = \sum_{j=0}^{L-1} e^{-ikj}(\tau_j - \bar{\tau})$ is the discrete spatial Fourier transform of the fluctuations of virtual time horizon. Then

$$\langle \hat{\tau}_i \hat{\tau}_{i+l} \rangle = \frac{1}{L} \sum_k e^{ikl} S^{(\tau)}(k) \quad (20)$$

and

$$\langle w^2(L, \infty) \rangle = \frac{1}{L} \sum_k S^{(\tau)}(k). \quad (21)$$

Since the universality class for the time horizon evolution is EW, it follows that the expected behavior for the steady-state structure factor for small wave-numbers is

$$S^{(\tau)}(k) \propto \frac{1}{k^2} \quad (22)$$

(see, e.g., Eq. (11) in Ref. [22]). Indeed, this is also confirmed by our direct simulation

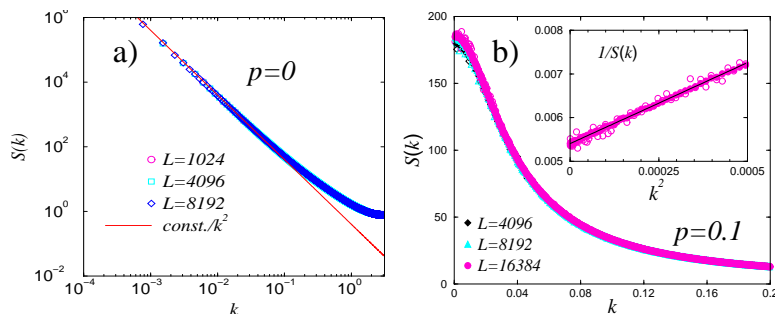


Figure 5: Steady-state structure factors for the virtual time horizon for the a) basic conservative scheme on a regular one-dimensional lattice ($p=0$) and b) for the small-world scheme with $p=0.1$.

results, shown Fig. 5a). This form of the structure factor implies that there are no length-scales other than the lattice constant and the systems size, and thus, the correlation length and the width diverge in the thermodynamic limit, as also can be seen by directly evaluating Eq. (21).

To de-correlate the surface fluctuations, we modify the communication topology in the following way [9]: for every node i , at the onset of the simulation, we introduce one extra quenched random communication link $r(i)$. Together with the existing regular topology, these extra communication links will form a small-world graph [26, 27, 28]. Note that in our specific construction of the small-world network, each node has exactly one random connection and $r(r(i))=i$, so that there are exactly $L/2$ random links distributed. The updating on PE i will obey the following probabilistically chosen condition:

$$\tau_i \leq \begin{cases} \min\{\tau_{i-1}, \tau_{i+1}, \tau_{r(i)}\} & \text{with probability } p \\ \min\{\tau_{i-1}, \tau_{i+1}\} & \text{with probability } 1 - p \end{cases}. \quad (23)$$

The PE *actually performs the update* (generate the virtual time of the next update, or deposit the rod at i in the MPEU surface) if condition (23) is fulfilled. This means that for sites that would normally be updated within the basic conservative scheme, i.e., $\tau_i \leq \min\{\tau_{i-1}, \tau_{i+1}\}$

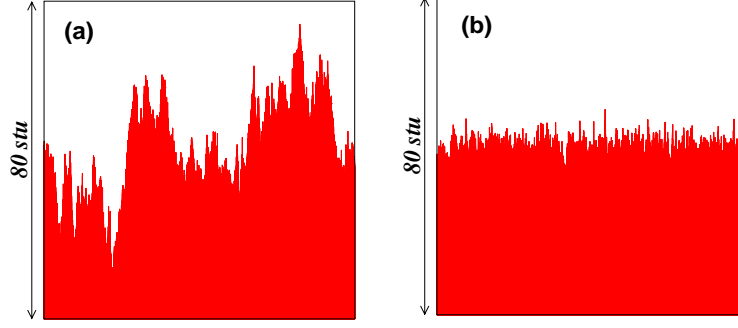


Figure 6: Steady-state virtual time horizon snapshots with $L = 10,000$ after $t = 10^6$ parallel algorithmic steps (Monte-Carlo sweeps) for a) the basic conservative scheme ($p = 0$) and b) the small-world scheme $p = 0.1$. Note that the vertical scales are the same in a) and b) (plotted in arbitrary simulated time units [stu]).

the PE will make an extra check for the condition $\tau_i \leq \tau_{r(i)}$ with probability p . The parameter p allows us to tune the scalability properties of the corresponding PDES scheme on the quenched small-world network continuously from the pure basic conservative scheme ($p = 0$) to the “fully” small-world conservative scheme ($p = 1$). These occasional extra

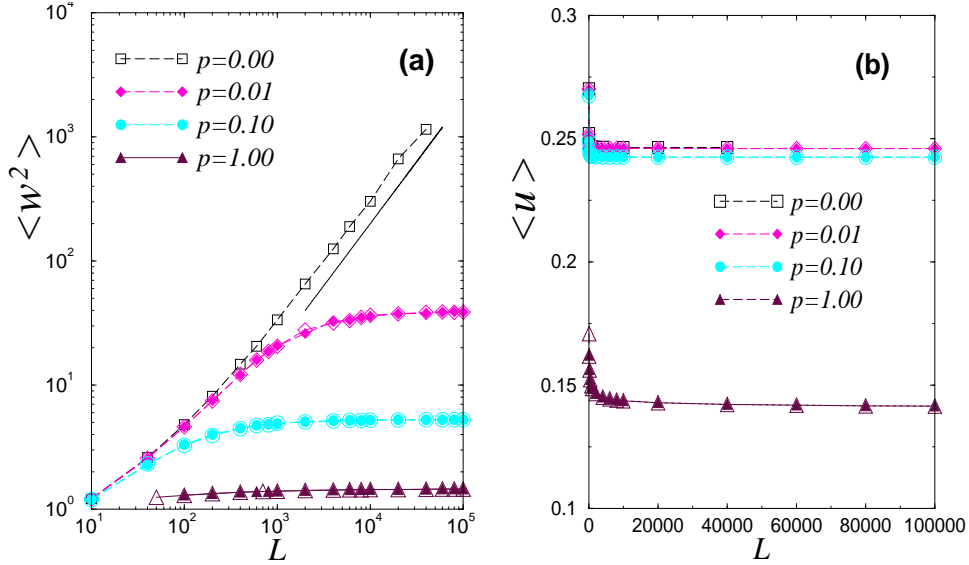


Figure 7: a) The average steady-state width and b) the utilization for various p values. In addition to ensemble averages over 10 realizations of the random links (solid symbols) a single realization is also shown (open symbols). The solid straight line has a slope of 1/2 and represents the asymptotic one-dimensional KPZ power-law divergence of the width for the basic conservative scheme ($p = 0$).

checkings through the quenched random links are not necessary for the faithfulness of the simulation. It is merely used to *synchronize* the PEs in such a way that the fluctuations of the time horizon remain bounded in the infinite system-size limit. Most importantly, as the width is reduced from “infinity” (or some large number proportional to L for finite number of PEs) to a finite controlled value, the utilization still remains bounded away from zero.

To support this statement, we first use the same coarse-graining procedure used to derive the KPZ equations as the continuum counterpart of the MPEU model. For the small-world topology we obtain

$$\frac{\partial \hat{\tau}}{\partial t} = -\gamma(p)\hat{\tau} + \frac{\partial^2 \hat{\tau}}{\partial x^2} - \lambda \left(\frac{\partial \hat{\tau}}{\partial x} \right)^2 + \xi(x, t). \quad (24)$$

with $\gamma(p) = 0$ for $p = 0$, and $\gamma(p) > 0$ for $0 < p \leq 1$. This implies that the extra checking along the random links introduces a *strong* relaxation (first term on the rhs of (24)) for the long-wavelength modes of the surface fluctuations, resulting in a finite width. A more transparent picture is gained if we look at the steady-state structure factor (19). Restricting our attention to the linear terms in Eq. (24) we obtain

$$S^{(\tau)}(k) \propto \frac{1}{\gamma + k^2}. \quad (25)$$

In this approximation, the lateral correlation length ξ_{\parallel} scales as $1/\sqrt{\gamma}$, and remains *finite* (and system-size independent) in the thermodynamic limit for all $p > 0$ (i.e., for an arbitrary small probability to utilize the random links). Figure 5b) shows the structure factor for the small-world network with $p = 0.1$, confirming the prediction of Eq. (25) for small wave numbers. Consequently, the height-height correlations decay exponentially

$$\langle \hat{\tau}_i \hat{\tau}_{i+l} \rangle \propto \xi_{\parallel} e^{-|l|/\xi_{\parallel}}, \quad (26)$$

and the width remains finite, $\langle w^2(L, \infty) \rangle \sim \xi_{\parallel}$, where ξ_{\parallel} is independent of the systems size for all $p > 0$. Further, for the structure factors of the local slopes (the Fourier transform of the slope-slope correlations) one obtains

$$S^{(\phi)}(k) = \frac{1}{L} \langle \tilde{\phi}_k \tilde{\phi}_{-k} \rangle = k^2 S^{(\tau)}(k) \propto \frac{k^2}{\gamma + k^2} = 1 - \frac{\gamma}{\gamma + k^2}. \quad (27)$$

Both terms above yield short-range correlations (delta function for the first term and exponential decay for the second one), thus, the slopes remain short-range correlated, resulting in a non-zero density of local minima. Figure 6 shows two snapshots of the virtual time horizons for the basic conservative scheme $p = 0$, and the small-world scheme with $p = 0.1$. Figure 7a) shows the scaling of the steady state width with the system size for various p values and Fig.7b) shows the scaling of the average, steady state utilization with the system size for the same set of p values. Notice that when increasing p (from $p=0$ to $p=0.01$), the width instantaneously drops from a linear divergence to a saturated value, while at the same time, the utilization hardly changes. In fact, an infinitesimally small p will make the width bounded, but at an only infinitesimal expense to the utilization. For example, for a hypothetically infinite system, taking $p=0.01$, the width is reduced from infinity to about 40, while the utilization from 0.2464 only to about 0.246; for $p=0.1$, the width is further reduced to about 5, while the utilization only to 0.242. By further increasing p , the width further reduces, and at $p=1$ it is about 1.46, whereas the utilization decreases to 0.141, still clearly bounded away from zero in the thermodynamic limit.

3 Scalability of the Conservative PDES-s scheme on scale-free network topologies

The Internet is a spontaneously grown collection of connected computers. The number of (only) webservers by February 2003 reached over 35 million [29]. The number of PC-s in use (Internet users) surpassed 660 million in 2002, and it is projected to surpass one billion by 2007 [30]. The idea for using it as a giant supercomputer is rather natural: many computers

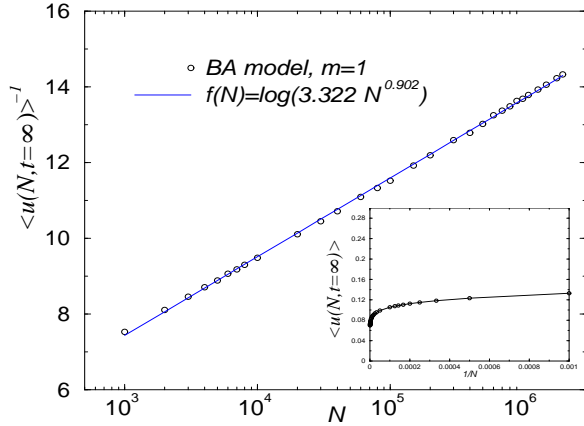


Figure 8: Steady-state utilization for the scale-free BA model.

are in an idle state, running at best some kind of screen-saver software, and the “waisted” computational time is simply immense. Projects such as SETI@home [31] or the GRID consortium [32] are targeting to harness the power lost in screen-savers.

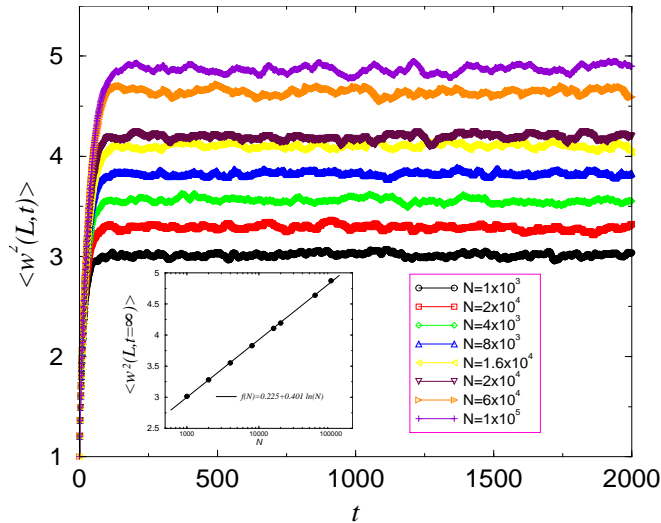


Figure 9: Behavior of the time horizon width for the scale-free BA network. The inset shows the scaling of the steady-state width as function of system size, N . Notice the log-lin scale on the inset.

Most of the problems solved currently with distributed computation on the Internet are “embarrassingly parallel” [33], i.e., the computed tasks have little or no connection to each

other similar to starting the same run with a number of different random seeds, and at the end collecting the data to perform statistical averages. However, before more large-scale, complex problems can be solved in real time on the Internet a number of challenges have to be solved, such as the task allocation problem which is rather complex by itself [11].

Here we ask the following question: *Given* that task allocation is resolved and the PE communication topology on the internet is a scale-free network, what are the scalability properties of a PDES-s scheme on such networks? Here we present numerical results, for the PDES-s update scheme, as measured on a model of scale-free networks, namely the Barabási-Albert model [34, 35]. This network is created through the stochastic process of preferential attachment: to the existing network at time t of N nodes, attaches the $N + 1$ -th node with m links (“stubs”) at time $t + 1$, such that each stub attaches to a node with probability proportional to the existing degree (at t) of the node. Here we will only present the $m = 1$ case, when the network is a scale-free tree. Once we reach a given number of nodes in the network, we stop the process and use the random network instance to run the MPEU model on top of it, using the evolution equation (8) for the time horizon. While in case of regular topologies, the degree of a node is constant, e.g. for d -dimensional “square” lattices, $P^{(L^d)}(k) = 2d\delta_{k,2d}$, for the BA network, it is a power law in the asymptotic ($N \rightarrow \infty$) limit : $P^{BA}(k) \simeq 2m^2k^{-3}$. The condition (1) for a site to be updated, i.e., that its virtual

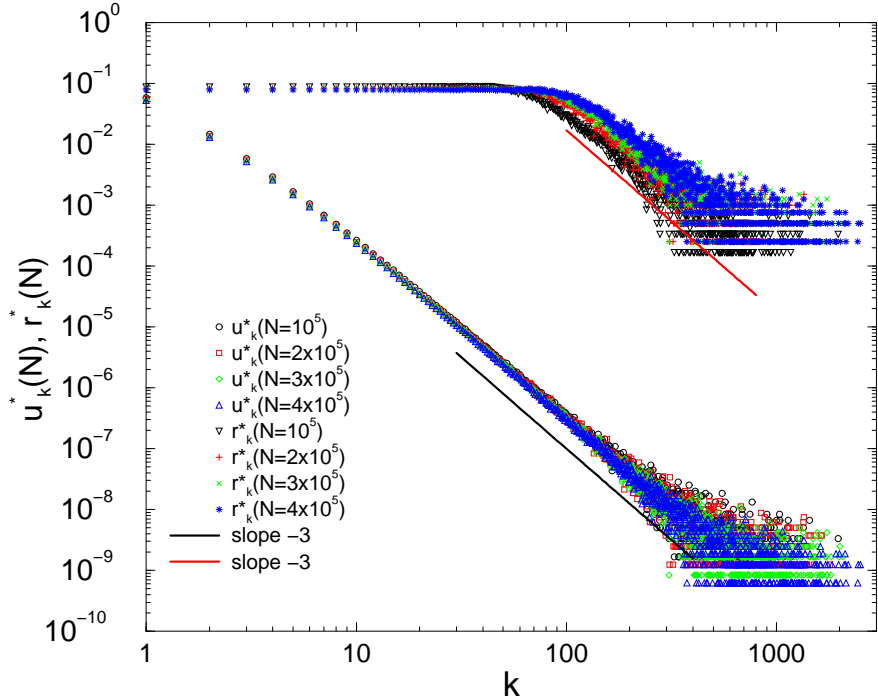


Figure 10: Connectivity-utilization u_k and relative connectivity utilization r_k as function of degree. Each data set is obtained after averaging over 200 independent runs.

time is a local minimum, is a *local* property, and thus we expect that the utilization itself be correlated with local structural properties of the graph, such as the degree distribution. To get a more detailed picture, we define two more quantities:

1) *connectivity-utilization*:

$$u_k(N, t) = \frac{|\mathcal{A}_k(t)|}{N} \quad (28)$$

which is the fraction of active nodes of degree k , and

2) the *relative connectivity-utilization*:

$$r_k(N, t) = \frac{|\mathcal{A}_k(t)|}{N_k} \quad (29)$$

which is the fraction of active nodes of degree k within the set of all nodes of degree k . From the above definitions we find the following obvious relations: $\sum_k u_k(N, t) = u(N, t)$ and $\sum_k r_k(N, t)N_k/N = \sum_k r_k(N, t)P^{BA}(k) = \sum_k u_k(N, t) = u(N, t) = \langle r_k(N, t) \rangle_{network}$ at all times. Figure 8 shows the steady state ($t \rightarrow \infty$, in the MPEU model on a fixed BA network of N nodes) values of the average utilization as function of the network size N . The inset in Fig. 8 is analogous to Fig. 3(a) which showed the same quantity on a ring. Notice that strictly speaking, the PDES-s scheme is computationally *non-scalable*. An empirical fit suggest that $u^*(N) = \langle u(N, t=\infty) \rangle \simeq [\ln(aN^b)]^{-1}$ with $a \simeq 3.322$ and $b = 0.902$, i.e., the computation is only logarithmically (or marginally) non-scalable. For a system of $N=10^3$ nodes we have found a steady state utilization (for the worst case scenario) of $u^*(10^3) = 0.1328$ (13.3% efficiency), while for a system of a million nodes, $N=10^6$, the utilization dropped only to $u^*(10^6) = 0.073$ (7.3% efficiency), by less than half of its value! For practical purposes the PDES-s scheme can be considered computationally scalable, and this type of non-scalability we will call *logarithmic* (or marginal) non-scalability.

Figure 9 shows the scaling of the width of the fluctuations for the time horizon as function of time, and the scaling of its value in the steady-state as function of system size (inset). Notice, that while the steady state width diverges to infinity, it only does so logarithmically, $\langle w^2(N, t=\infty) \rangle \simeq [\ln(cN^d)]$ with $c \simeq 1.25$ and $d \simeq 0.401$. Some specific values: $\langle w^2(10^3, t=\infty) \rangle \simeq 3.01$, $\langle w^2(10^5, t=\infty) \rangle \simeq 4.78$. This means that the measurement phase of the PDES-s scheme on a scale-free network is non-scalable either, however, it is so only logarithmically, and for practical purposes the scheme can be considered scalable. Overall, the PDES-s update scheme has logarithmic (or marginal) non-scalability on scale-free networks. If one examines the connectivity-utilization and relative connectivity-utilization in the steady state, as shown in Fig. 10, one finds that with good approximation $u_k^*(N) \sim k^{-3}$, and $r_k^*(N) = const. \simeq u^*(N)$ for $k \leq k_\times$ and $r_k^*(N) \sim k^{-3}$ for $k > k_\times$, with $k_\times \sim 1/u^*(N) = \ln(aN^b) \sim \ln N$, being a crossover degree.

4 Conclusions

We studied the fundamental scalability problem of conservative PDES schemes where events are self-initiated and have identical distribution on each PE. First, we considered the scalability of the basic conservative scheme for systems with short-range interactions on regular lattices. By exploiting a mapping [8] between the progress of the simulation and kinetic roughening in non-equilibrium surfaces, we found that while the average progress rate of the PEs $\langle u(\infty, \infty) \rangle$ is a finite *non-zero* value, the spread of the progress of the PEs about the mean $\langle w^2(\infty, \infty) \rangle$ *diverges*. The former property makes the measurement phase of the

algorithm non-scalable. In order to make the measurement part of the simulation scalable as well, we introduced [9] quenched random connections between PEs (exactly one for each) so that the resulting random links on the top of the regular short-range connections formed a *small-world*-like connection topology. Invoking the same conservative protocol used at an arbitrarily small rate through the random links was sufficient to achieve full scalability: the PEs progress at a non-zero, near uniform rate *without* requiring global synchronization [9]. The above construction of a fully scalable algorithm for simulating large systems with asynchronous dynamics and short-range interactions is an example for the enormous “computational power and synchronizability” [26] that can be achieved by small-world couplings. The suppression of critical fluctuations of the virtual time horizon is also closely related to the emergence of mean-field-like phase transitions and phase ordering in *non-frustrated* interacting systems [37, 38, 39, 40, 41]. In particular, the fluctuations exhibited by the virtual time horizon with small-world synchronization should exhibit very similar characteristics to the fluctuations of the order parameter in the XY-model placed on a small-world network [39].

Second, we studied the scalability properties for a causally constrained PDES scheme hosted by a network of computers where the network is *scale-free* following a “preferential attachment” construction [34, 35]. Here the PEs simply have to satisfy the general criterion Eq. (1) in order to advance their local time. Despite some nodes in the network having abnormally large connectivity (as a result of the scale-free nature of the degree distribution), we found that the computational phase of the algorithm is only marginally non-scalable. The utilization exhibited slow logarithmic decay as a function of the number of PEs. At the same time, the width of the time horizon diverged logarithmically slowly, rendering the measurement phase of the simulations marginally non-scalable as well. An intriguing question to pursue is how the logarithmic divergence of the surface fluctuations observed here can be related to the collective behavior (in particular, the finite-size effects of the magnetic susceptibility) of Ising ferromagnets on scale-free networks [42, 43, 44, 45] with the same degree distribution.

Acknowledgements

Discussions with P.A. Rikvold, B.D. Lubachevsky, Z. Rácz and G. Istrate are gratefully acknowledged. Z.T. was supported by the DOE under contract W-7405-ENG-36. This research is supported in part by NSF through Grant No. DMR-0113049 and the Research Corporation through Grant No. RI0761.

References

- [1] R. Fujimoto, *Commun. ACM* **33**, 30 (1990).
- [2] D.M. Nicol, R.M. Fujimoto, *Ann. Oper. Res.* **53**, 249 (1994).
- [3] B.D. Lubachevsky, *Bell Labs Tech. J.* **5** April-June 2000, 134 (2000).

- [4] R.E. Felderman and L. Kleinrock. Bounds and Approximations for Self-Initiating Distributed Simulation without Lookahead. *ACM Trans. Model. Comput. Simul.* **1**, 386 (1991).
- [5] B.D. Lubachevsky, *Complex Syst.* **1**, 1099 (1987).
- [6] B.D. Lubachevsky, *J. Comput. Phys.* **75**, 103 (1988).
- [7] G. Korniss, M.A. Novotny and P.A. Rikvold, *J. Comput. Phys.* **153**, 488 (1999).
- [8] G. Korniss, Z. Toroczkai, M.A. Novotny and P.A. Rikvold, *Phys. Rev. Lett.* **84**, 1351 (2000).
- [9] G. Korniss, M.A. Novotny, H. Guclu, Z. Toroczkai and P.A. Rikvold, *Science* **299**, 677 (2003).
- [10] P.M.A. Sloot, B.J. Overeinder, A. Schoneveld, *Comput. Phys. Commun.* **142**, 76 (2001).
- [11] A. Schoneveld, *Parallel Complex Systems Simulation* Ph.D. Thesis, Universiteit van Amsterdam, (1999).
- [12] D.R. Jefferson, *ACM Trans.Prog.Lang.Syst.* **7**, 404 (1985).
- [13] P. Bak, C. Tang and K. Wiesenfeld, *Phys.Rev.Lett.* **59**, 381 (1987).
- [14] K.M. Chandy, J. Misra, *Commun. ACM* **24**, 198 (1981).
- [15] A.G. Greenberg, B.D. Lubachevsky, D.M. Nicol and P.E. Wright, in *Proceedings of the 8th Workshop on Parallel and Distributed Simulations (PADS'94)*, Edinburgh, UK, 1994 (Society for Computer Simulation, San Diego, CA, 1994), p. 187.
- [16] Z. Toroczkai, G. Korniss, in preparation.
- [17] M. Burgers, *The Nonlinear Diffusion Equation* (Riedel, Boston, 1974).
- [18] M. Kardar, G. Parisi and Y.-C. Zhang, *Phys. Rev. Lett.* **56**, 889 (1986).
- [19] A.-L. Barabási and H.E. Stanley, *Fractal Concepts in Surface Growth*, (Cambridge Univ. Press, 1995)
- [20] J. Krug and P. Meakin, *J. Phys. A* **23**, L987 (1990).
- [21] G. Foltin, K. Oerding, Z. Rácz, R.L. Workman and R.K.P. Zia, *Phys.Rev.E* **50**, R639 (1994).
- [22] Z. Toroczkai, G. Korniss, S. Das Sarma and R.K.P. Zia, *Phys. Rev.E*, **62**, 276 (2000).
- [23] G. Korniss, M.A. Novotny, P.A. Rikvold, H. Guclu, and Z. Toroczkai, *Mat. Res. Soc. Symp. Proc.*, **700**, 297 (2002).
- [24] G. Korniss, M.A. Novotny, Z. Toroczkai, and P.A. Rikvold in *Computer Simulated Studies in Condensed Matter Physics XIII*, Eds: D.P. Landau, S.P. Lewis and H.-B. Schüttler, Springer-Verlag Berlin Heidelberg (2001), pp. 183.

- [25] A.K. Kolakowska, M.A. Novotny, G. Korniss, “Algorithmic scalability in globally constrained conservative parallel discrete event simulations of asynchronous systems”, *Phys. Rev. E* **67**, 046703 (2003).
- [26] D.J. Watts, S.H. Strogatz, *Nature* **393**, 440 (1998).
- [27] M.E.J. Newman, D.J. Watts, *Phys. Lett. A* **263**, 341 (1999).
- [28] J. Kleinberg, *Nature* **406**, 845 (2000).
- [29] www.netcraft.com/survey/
- [30] www.c-i-a.com/
- [31] setiathome.ssl.berkeley.edu
- [32] www.gridforum.org
- [33] S. Kirkpatrick, *Science* **299**, 668 (2003)
- [34] A.L. Barabási, R. Albert, *Science*, **286**, 509 (1999)
- [35] A.L. Barabási, R. Albert, and H. Jeong, *Physica A*, **272**, 173 (1999).
- [36] S.H. Strogatz: *Nature* **410**, 268 (2001)
- [37] A. Barrat, M. Weigt, *Eur. Phys. J. B* **13**, 547 (2000).
- [38] M. Gitterman, *J. Phys. A* **33**, 8373 (2000).
- [39] B.J. Kim et al, *Phys. Rev. E* **64**, 056135 (2001).
- [40] H. Hong, B.J. Kim, M.Y. Choi, *Phys. Rev. E* **66**, 018101 (2002).
- [41] H. Hong, M.Y. Choi, B.J. Kim, *Phys. Rev. E* **65**, 047104 (2002).
- [42] A. Aleksiejuk, J.A. Holyst, D. Stauffer, *Physica A* **310**, 260 (2002).
- [43] M. Leone, A. Vázquez, A. Vespignani, R. Zecchina, *Eur. Phys. J. B* **28**, 191 (2002).
- [44] S.N. Dorogovtsev, A.V. Goltsev, J.F.F. Mendes, *Phys. Rev. E* **66**, 016104 (2002).
- [45] G. Bianconi, *Phys. Lett. A* **303**, 166 (2002).